Inflammatory cytokine signaling in insulin producing ß-cells enhances the colocalization correlation coefficient between L-type voltage-dependent calcium channel and calcium-sensing receptor

JAI PARKASH

Robert Stempel School of Public Health, Department of Environmental and Occupational Health, Florida International University, 11200 SW 8th Street, Miami, FL 33199, USA

Received February 11, 2008; Accepted March 26, 2008

DOI: 10.3892/ijmm_00000003

Abstract. The immunological processes in type 1 diabetes and metabolic/inflammatory disorder in type 2 diabetes converge on common signaling pathway(s) leading to ß-cell death in these two diseases. The cytokine-mediated ß-cell death seems to be dependent on voltage-dependent calcium channel (VDCC)-mediated Ca^{2+} entry. The Ca^{2+} handling molecular networks control the homeostasis of $[Ca^{2+}]_i$ in the ß-cell. The activity and membrane density of VDCC are regulated by several mechanisms including G protein-coupled receptors (GPCRs). CaR is a 123-kDa seven transmembrane extracellular Ca^{2+} sensing protein that belongs to GPCR family C. Tumor necrosis factor-α (TNF-α), is a cytokine widely known to activate nuclear factor-κB (NF-κB) transcription in ß-cells. To obtain a better understanding of TNF-α-induced molecular interactions between CaR and VDCC, confocal fluorescence measurements were performed on insulin-producing ß-cells exposed to varying concentrations of TNF-α and the results are discussed in the light of increased colocalization correlation coefficient. The insulin producing ß-cells were exposed to 5, 10, 20, 30, and 50 ng/ml TNF-α for 24 h at 37˚C. The cells were then immunolabelled with antibodies directed against CaR, VDCC, and NF-κB. The confocal fluorescence imaging data showed enhancement in the colocalization correlation coefficient between CaR and VDCC in ß-cells exposed to TNF-α thereby indicating increased membrane delimited spatial interactions between these two membrane proteins. TNF-α-induced colocalization of VDCC with CaR was inhibited by nimodipine, an inhibitor of L-type VDCC thereby suggesting that VDCC activity is required for spatial interactions with CaR. The 3-D confocal fluorescence imaging data also demonstrated that addition of TNF-α to RIN cells led to the translocation of NF-κB from the cytoplasm to the nucleus. Such molecular interactions between CaR and VDCC in tissues possibly provide control over Ca^{2+} channel activity via direct protein-protein contact.

Correspondence to: Dr Jai Parkash, Robert Stempel School of Public Health, Department of Environmental and Occupational Health, Room HLS-594, Florida International University, 11200 SW 8th Street, Miami, FL 33199, USA
E-mail: parkashj@fiu.edu

Key words: ß-cells, calcium-sensing receptor, colocalization correlation coefficient, diabetes, inflammation, L-type voltage-dependent calcium channel, nuclear factor-κB, tumor necrosis factor-α

Introduction

The programmed cell death (apoptosis) of insulin producing ß-cells is a common characteristic of type 1 and type 2 diabetes mellitus. In type 1 diabetes, anti-ß-cell autoimmune reactions and associated inflammations lead to ß-cell death. In type 2 diabetes, the metabolic disorder is associated with the production of inflammatory cytokines in insulin-sensitive tissues leading to elevated levels of circulating inflammatory cytokines such as interleukin-6 (IL-6) and tumor necrosis factor-alpha (TNF-α). The immunological processes in type 1 diabetes and metabolic/inflammatory disorder in type 2 diabetes converge on common signaling pathway(s) leading to ß-cell death in these two diseases.

Cytokine-mediated ß-cell death seems to be dependent on voltage-dependent calcium channel (VDCC)-mediated Ca^{2+} entry as suggested by the findings that blockers of L-type VDCC can suppress ß-cell apoptosis induced by IL-1ß (1,2) or IFNγ plus TNF-α (3), and blockers of T-type VDCC can repress ß-cell apoptosis induced by a mixture of cytokines (4). The L-type VDCC is a VDCC major subtype found in the ß-cells of most species and is expressed in all the primary ß-cells and insulin-secreting cell lines (5,6). The spatio-temporal regulation of $[Ca^{2+}]_i$ in the ß-cell is dependent upon the functioning of several molecular entities in which VDCCs play major roles (7). VDCC activity and distribution within the cell are regulated by various molecular complexes such as Ca^{2+}/calmodulin, G protein-coupled receptors (GPCRs), protein kinases, and inositol phosphates (5). VDCC gene expression changes in response to several physiological stimuli and pathological conditions. Cytokine incubation can turn on the gene expression of CaV3 channels in mouse ß-cells (4).

Calcium-sensing receptor (CaR) is a 123-kDa seven transmembrane extracellular Ca^{2+} sensing protein that resides within caveolin-rich membrane domains and belongs to GPCR family C (8,9). CaR is activated by Ca^{2+}, divalent and

trivalent cations, polycations, amino acids, and polyamines (8,10,11). CaR is also expressed in human islets and in human insulinoma cells (12-14). The CaR protein regulates several cellular processes including gene expression, cell proliferation and differentiation, secretion, and apoptosis (8). Although, the role of CaR in insulin secretion is still not fully understood, CaR may participate in ß-cell replication and differentiation, thus regulating nutrient-induced insulin secretion, and could, therefore, be a potential target for the treatment of diabetes (11,13-16).

The GPCRs interact with many other intracellular proteins in addition to G proteins, such as ion channels, chaperone and trafficking proteins, scaffolding and structural proteins, signaling proteins, and a regulator of G protein signaling (17-20). The C-terminus of the CaR has been shown to interact with and inactivate two inwardly rectifying K channels, Kir4.1 and Kir4.2, in the kidney that are expressed in the distal nephron (thick ascending limb of Henle and distal convoluted tubule) as well as other tissues (21).

We showed previously that TNF-α can decrease intracellular Ca^{2+} buffering capacity by decreasing the levels of a high affinity calcium-binding protein and thus increase the rate of ß-cell apoptosis in a transformed insulin-secreting ß-cell line, rat insulinoma (RIN) cells (22). The same study also demonstrated that calcium influx in response to KCl and ionomycin is larger in RIN cells (ß-cells) that have been previously exposed to TNF-α (22). TNF-α is a cytokine widely known to activate NF-κB transcription in ß-cells (23-25). Cytokines can induce ß-cell apoptosis through the induction of signaling pathways that activate NF-κB (26-28). NF-κB is usually stored in the cytosol in its inactive form, bound to the inhibitory unit IκBα, which prevents DNA binding and nuclear translocation. NF-κB activating agents initiate phosphorylation of IκBα, inducing polyubiquitination at multiple sites and tagging the subunit for degradation by a 26S proteosome complex (26-28). To obtain a better understanding of TNF-α-induced molecular interactions between CaR (a GPCR) and VDCC (a voltage-gated channel) confocal fluorescence measurements were performed on insulin-producing ß-cells exposed to varying concentrations of TNF-α; the results are described herein and discussed in light of the colocalization correlation coefficient.

Materials and methods

Cell culture. Rat insulinoma cells, RINr 1046-38 (RIN), insulin-producing ß-cells, kindly provided by Dr Bruce Chertow (Veterans Administration Medical Center, Huntington, WV, USA), were grown on 25-mm diameter glass coverslips in six-well culture plates in a 5% CO_2 incubator at 37°C. The cell culture medium was RPMI-1640 supplemented with 10% (w/v) fetal bovine serum, 100 units/ml of penicillin, and 100 μg/ml of streptomycin (Invitrogen Corporation, Grand Island, NY, USA).

Treatment with TNF-α. After 5 days of culture, RIN cells were treated with 5, 10, 20, 30, and 50 ng/ml TNF-α (rat, recombinant; Chemicon International, Temecula, CA) directly added to the cell culture medium and the cells were allowed to grow for the next 24 h at 37°C.

Immunofluorescence labeling. RIN cells were washed thrice and fixed with Bouin solution (Sigma Chemical Company, St. Louis, MO, USA) for 30 min at room temperature. The cells were then washed thrice with phosphate-buffer saline (PBS) followed by dehydration with 50, 70, 95, and finally 100% ethanol (EtOH) in PBS. The cells were then rehydrated by using 100, 95, 70, and 50% EtOH, and finally 0% EtOH (i.e. PBS). The hydrated RIN cells were permeabilized with 0.2% Triton X-100 (Sigma Chemical Company) at room temperature for 10 min and again washed thrice with PBS. To block non-specific binding of antibodies, the RIN cells were first blocked thrice for 5 min each with the blocking buffer containing 2% bovine serum albumin (BSA) in PBS followed by blocking with 5% normal goat serum in blocking buffer for 30 min. The RIN cells were then treated for 1 h at room temperature with i) an affinity purified goat polyclonal antibody raised against a peptide mapping within a C-terminal cytoplasmic domain of CaR of human origin (Santa Cruz Biotechnology, Inc., USA) and ii) an affinity purified rabbit antibody (Anti-Cav1.2) raised against a peptide corresponding to residues 844-865 of rat L-type VDCC, Cav1.2 (α_1C) (Alomone Labs Ltd, Israel) or iii) an affinity purified polyclonal antibody raised against a peptide mapping at the C-terminus of NF-κB of human origin (Santa Cruz Biotechnology) wherever needed (see Results). The concentrations of primary antibodies solutions were 1 μg/ml and the solutions were prepared in blocking buffer, centrifuged at 13000 x g for 10 min before use. Following primary antibody treatment, the cells were washed thrice with blocking buffer and then treated with 5 μg/ml of Alexa Fluor 488 goat anti-rabbit IgG and Alexa Fluor 546 donkey anti-goat IgG fluorescent secondary antibodies (Invitrogen, Molecular Probes, Eugene, OR, USA) for 1 h at room temperature. The cells were then washed thrice with blocking buffer and thrice with PBS and the coverslips were mounted onto glass slides using water soluble Fluoromont-G (SouthernBiotech, Birmingham, AL, USA).

Confocal fluorescence microscopy. The confocal fluorescence images were scanned on a Nikon TE2000U inverted fluorescence microscope equipped with a Nikon D-Eclipse C1 laser scanning confocal microscope system (Nikon Corp., USA). The z-series scans were performed at every micrometer up to a z-depth of 10 μm by using a Nikon 40 x 1.30 NA DIC H/N2 Plan Fluor oil immersion objective. The 488-nm excitation beam was generated with a Spectra-Physics (Mountain View, CA, USA) argon laser and the 543-nm excitation beam was provided with a Melles Griot (Carlsbad, CA, USA) Helium-Neon laser. The built-in Nikon EZ-C1 software and Metamorph 6 software (Universal Imaging Corp., USA) were used for confocal image acquisition and analyses.

Confocal image analysis and calculation of colocalization correlation coefficient of VDCC with CaR. The 3-D confocal images obtained were processed with Nikon EZ-C1 software as described above and imported into Metamorph 6 software for further analysis. In order to determine the colocalization of VDCC with CaR, the confocal images were color thresholded for green (VDCC) and red (CaR). The colocalization correlation coefficients were measured by using the Correlation

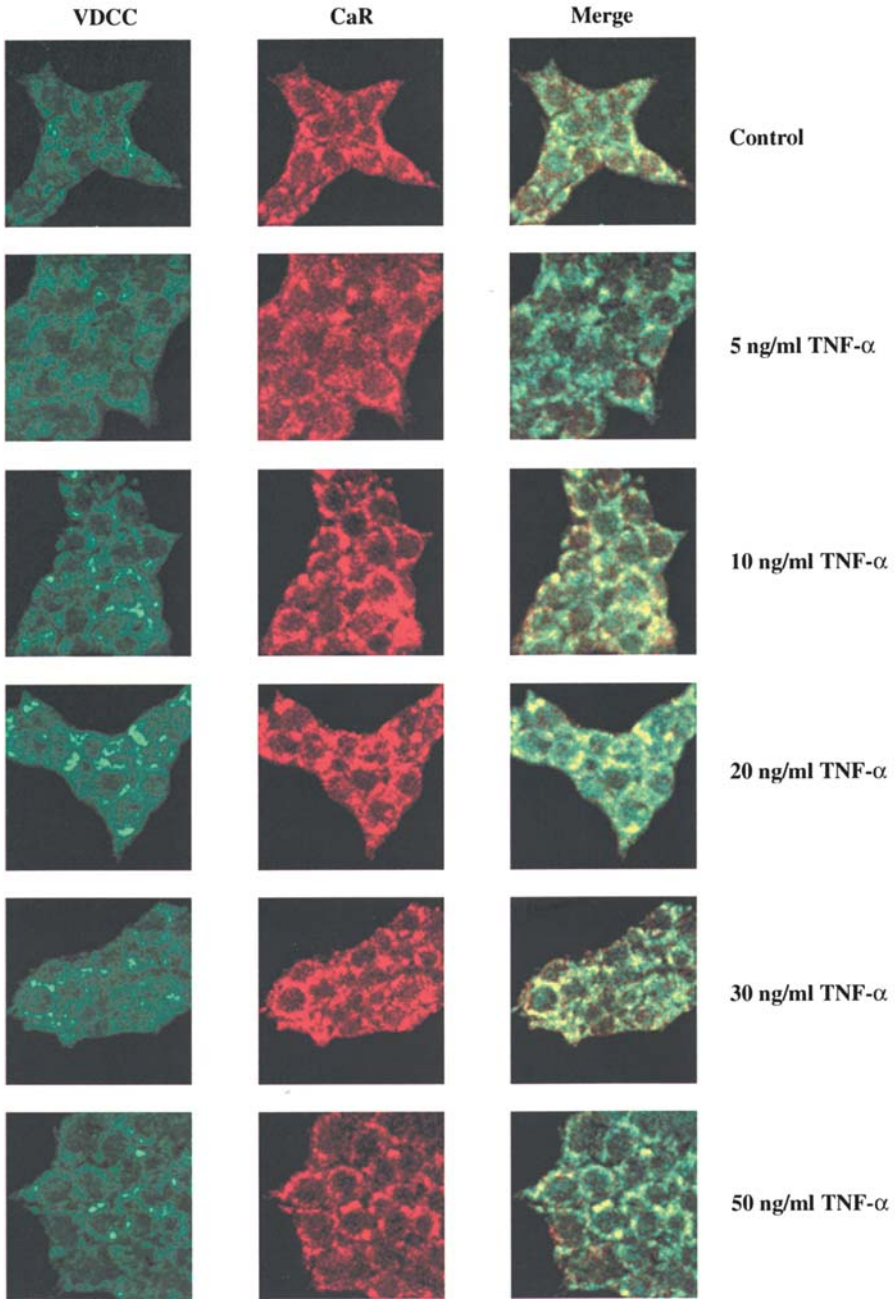

Figure 1. Insulin producing ß-cells were treated with increasing concentrations of TNF-α. The confocal immunofluorescence imaging data shows increased spatial interaction between VDCC (shown in green, left panel) and CaR (shown in red, middle panel) as indicated by the appearance of yellow color in the merged images (right panel).

Plot plug-in available in the Metamorph 6 software (29,30). The correlation coefficient (r) of the data was defined as:

$$r = \sum xy / NS_xS_y$$

where r = correlation coefficient, xy = product of deviation scores, N = sample size, S_x = standard deviation of X (intensities in first image), and S_y = standard deviation of Y (intensities in second image). The theoretical range of values of the correlation coefficient was -1.0 to +1.0, wherein a value of 1.0 indicates that the data were perfectly correlated with one another. This would only occur in the case of two identical images. A correlation coefficient of -1.0 would result in the case of an inverse relationship between the intensities of two images.

Nuclear translocation of NF-κB induced by TNF-α. The ratio of localization of NF-κB in nuclear to cytoplasmic regions was determined by measuring the integrated fluorescence intensities in the nuclear and cytoplasmic regions of 3-D confocal fluorescence images of RIN cells acquired by using the Nikon C-1 confocal system as described above, and further analysis of these images with Metamorph 6.

Results

The insulin producing ß-cells were exposed to 5, 10, 20, 30, and 50 ng/ml TNF-α for 24 h at 37˚C. The cells were then immunolabelled with antibodies directed against CaR and VDCC or NF-κB as described above in Materials and methods.

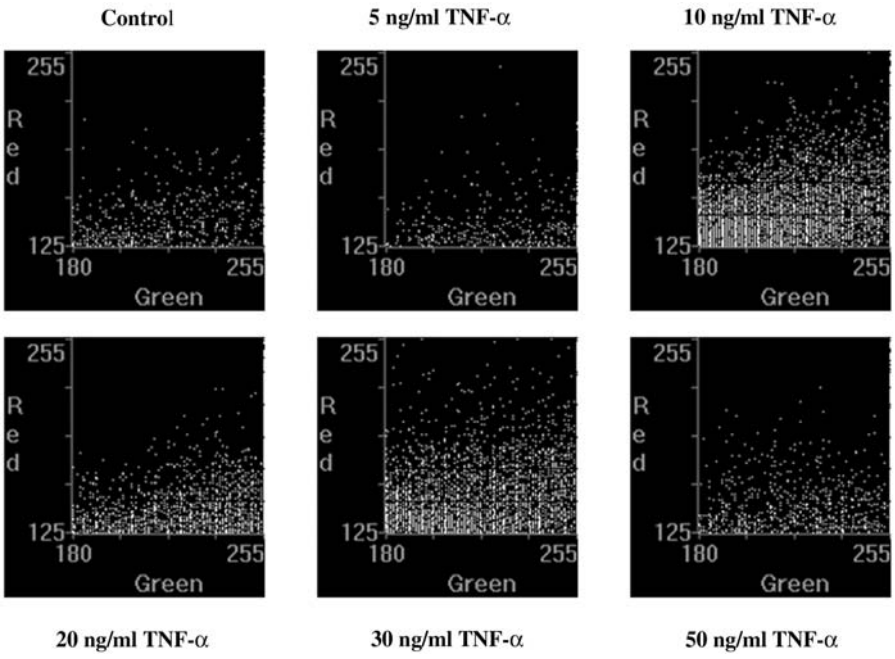

Figure 2. Correlation plots showing CaR pixels on Y-axis (red) and VDCC pixels on X-axis (green) in control and TNF-α-treated RIN cells indicating increased spatial interactions between these two membrane proteins in the TNF-α-treated RIN cells.

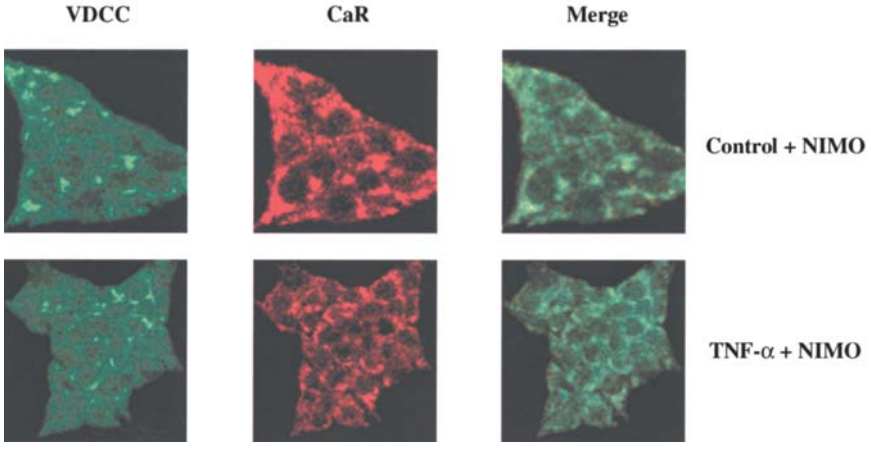

Figure 3. Insulin producing ß-cells were pretreated with 10 μM NIMO, an inhibitor of L-type VDCC, followed by incubation with 10 ng/ml TNF-α. The confocal immunofluorescence imaging data suggest inhibition of spatial interaction between VDCC (shown in green, left panel) and CaR (shown in red, middle panel) as indicated by the absence of any yellow color in the merged images (right panel). The data indicate that VDCC activity is required for spatial interaction between CaR and VDCC.

The 3-D confocal fluorescence images showing VDCC (left panel, in green) and CaR (middle panel, in red) as well as the merged images (right panel) are presented in Fig. 1. It is evident from Fig. 1 that the addition of TNF-α to the RIN cells resulted in increased colocalization of CaR with VDCC as shown by the presence of yellow color in the merged images (right panel). In order to provide a mathematical definition for this colocalization of CaR with VDCC and also to measure the degree of colocalization, the data presented in Fig. 1 were further analyzed by calculating the colocalization correlation coefficient (see Materials and methods) and the results are presented in Table I. In control RIN cells, the correlation coefficient was 0.2766 whereas in TNF-α-treated RIN cells at 5 and 30 ng/ml the correlation coefficient decreased by 25 and 17% respectively as compared to that in control RIN cells (Table I, column 3). However, at 10, 20, and 50 ng/ml TNF-α, significant increases in the correlation coefficient by 28, 75, and 18% respectively, were observed (Table I, column 3). The data showed that at 20 ng/ml TNF-α, the correlation coefficient increased by 75% thereby indicating the maximum colocalization of CaR with VDCC. The theoretical range of values for the correlation coefficient was -1.0 to +1.0 wherein a value of 1.0 indicates a perfect correlation of data which would only occur in the case of two identical images or the complete colocalization of the two proteins, and a value of -1.00 indicates an inverse relationship

Table I. Effect of TNF-α on the colocalization correlation coefficient.[a]

Sample	Correlation coefficient (r)	Relative r (%)
Control	0.2766	100
5 ng/ml TNF-α	0.2073	75
10 ng/ml TNF-α	0.3531	128
20 ng/ml TNF-α	0.4829	175
30 ng/ml TNF-α	0.2296	83
50 ng/ml TNF-α	0.3250	118
Control + 10 μM NIMO	0.1805	65
10 μM NIMO + 10 ng/ml TNF-α	0.0000	0

[a]The correlation coefficient (r) of the data is defined as: $r = \sum xy / NS_xS_y$, where: r = correlation coefficient, xy = product of deviation scores, N = sample size, S_x = standard deviation of X (intensities in first image), and S_y = standard deviation of Y (intensities in second image). The range of values of the correlation coefficient is -1.0 to +1.0. A value of 1.0 would indicate that the data are perfectly correlated with one another which would only occur in the case of two identical images. A correlation coefficient of -1.0 would result in the case of an inverse relationship between the intensities of two images.

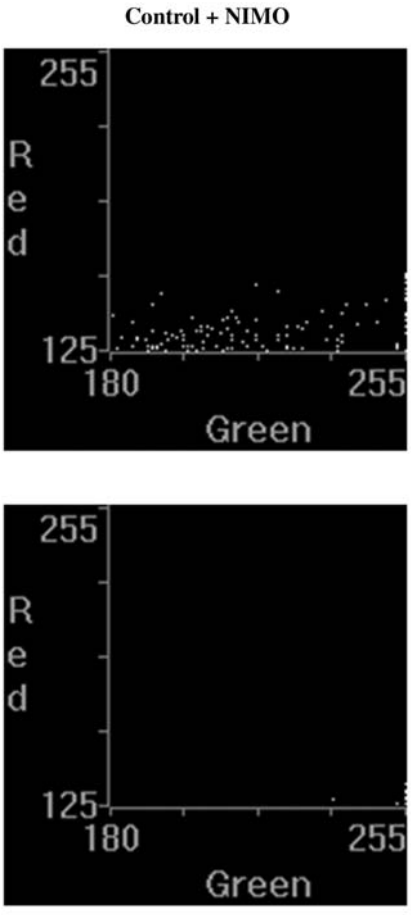

Figure 4. Correlation plots showing CaR pixels on Y-axis (red) and VDCC pixels on X-axis (green) in control RIN cells pretreated with 10 μM NIMO and TNF-α-treated RIN cells pretreated with 10 μM NIMO indicating a significant inhibition of spatial interactions between these two membrane proteins particularly in TNF-α-treated RIN cells.

between pixel intensities in the two images thereby suggesting the absence of colocalization between the two proteins. The correlation plots showing CaR pixel intensities (red, on Y-axis) and VDCC (green, on X-axis) are shown for control and TNF-α treated RIN cells in Fig. 2. These correlation plots are a visual demonstration, in terms of pixel intensities, of the correlation plots between CaR (in red, Y-axis) and VDCC (green, X-axis) in control, and in 5, 10, 20, 30, and 50 ng/ml TNF-α-treated RIN cells. It is evident from these plots that the presence of a cytokine such as TNF-α induces increased spatial interactions between CaR and VDCC.

In order to test whether TNF-α-induced colocalization of VDCC with CaR could be inhibited by the activity of L-type VDCC, the RIN cells were first incubated with 10 μM nimodipine (NIMO), an inhibitor of L-type VDCC, followed by incubation of RIN cells with no TNF-α (control) and 10 ng/ml TNF-α for 24 h at 37˚C. Fig. 3 shows the results for VDCC (left panel, in green), CaR (middle panel, in red) and merged images (right panel). The 3-D confocal fluorescence imaging data presented in Fig. 3 indicate that the addition of 10 μM NIMO inhibited the spatial interaction between CaR and VDCC both in control and in TNF-α-treated RIN cells since no yellow color was observed in the merged images (right panel). This finding is further supported by the results for the colocalization correlation coefficient measurement. As shown in Table I, the addition of 10 μM NIMO to control RIN cells resulted in a 35% decrease in the correlation coefficient and most importantly the pretreatment of RIN cells with 10 μM NIMO, followed by addition of 10 ng/ml TNF-α significantly inhibited the interaction between CaR and VDCC since the correlation coefficient result was 0.0000. This is further substantiated by the correlation plots in Fig. 4 that show CaR (red, on Y-axis) and VDCC (green, on X-axis) for control and TNF-α-treated RIN cells and indicate the inhibitory effect of VDCC inhibitor NIMO on spatial interaction between CaR and VDCC, thereby suggesting that VDCC activity is required for spatial interactions.

In order to demonstrate that the addition of TNF-α leads to the translocation of NF-κB from the cytoplasm to the nucleus, the control and TNF-α-treated RIN cells were immunolabelled with antibody directed against the p65 subunit of NF-κB and the confocal immunofluorescence microscopy measurements were carried out as described in detail in Materials and methods. The 3-D confocal fluorescence images presented in Fig. 5 show that the addition of TNF-α to RIN cells led to the translocation of NF-κB from the cytoplasm to the nucleus. In order to accord a mathematical value to the nuclear translocation of NF-κB, the ratio of fluorescence intensities in the nuclear and cytoplasmic regions was calculated and the results are presented in Table II. These results indicate that the addition of TNF-α to RIN cells significantly increased the nuclear translocation of NF-κB as defined by a more than 3-fold increase in the fluorescence ratios. In the presence of 10 μM NIMO, the increase in the

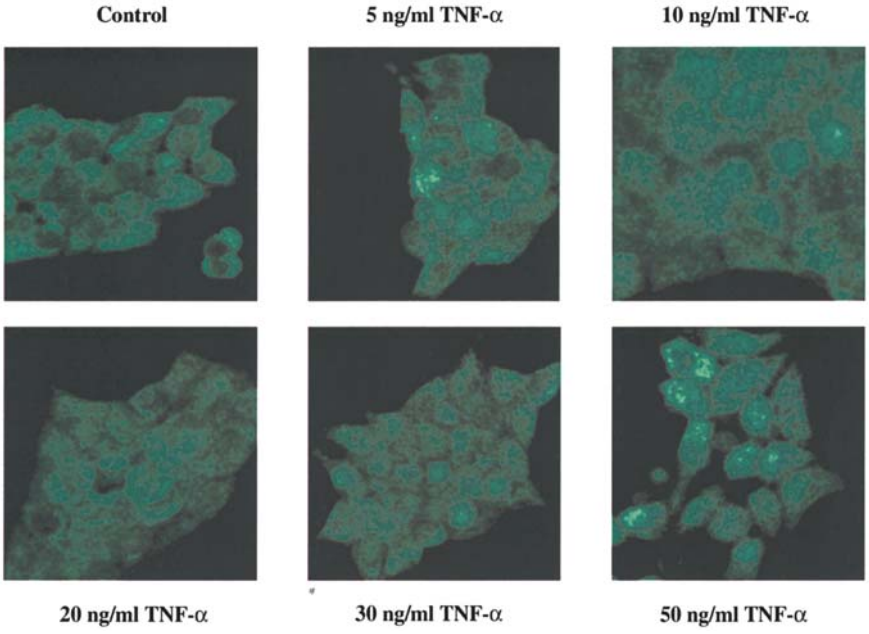

Figure 5. 3-D confocal immunofluorescence images showing the localization and nuclear translocation of NF-κB in control and TNF-α-treated RIN cells. The data indicate increased nuclear translocation of NF-κB in TNF-α-treated RIN cells (see Table II also).

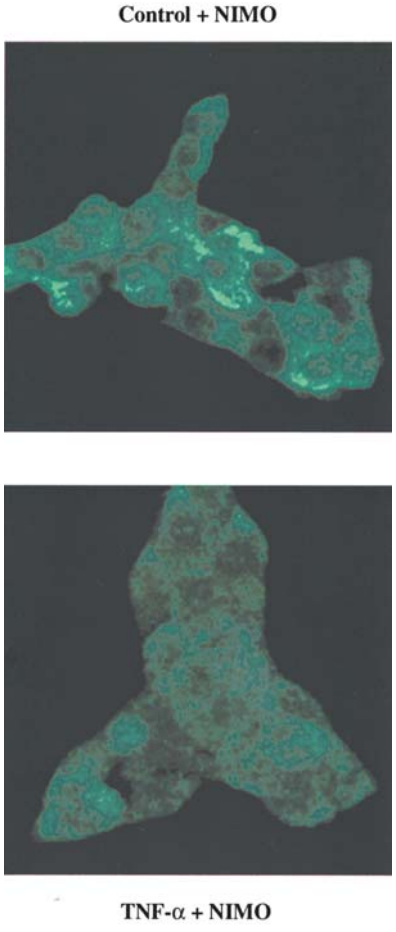

Figure 6. 3-D confocal immunofluorescence images showing the localization and nuclear translocation of NF-κB in control RIN cells pretreated with 10 μM NIMO and TNF-α-treated RIN cells pretreated with 10 μM NIMO.

Table II. Nuclear translocation of NF-κB induced by TNF-α.

Sample	Ratio[a]	Relative ratio (%)
Control	0.3360	100
5 ng/ml TNF-α	0.7320	218
10 ng/ml TNF-α	1.0350	308
20 ng/ml TNF-α	1.0790	321
30 ng/ml TNF-α	1.0780	321
50 ng/ml TNF-α	0.7609	226
Control + 10 μM NIMO	0.7350	219
10 μM NIMO + 10 ng/ml TNF-α	0.8390	250

[a]The fluorescence ratio is defined as: Integrated fluorescence intensity in nucleus / Integrated fluorescence intensity in cytoplasm. The NF-κB localization was determined by using immunofluorescence with a primary antibody against the p65 subunit of NF-κB and the secondary antibody was labeled with Alexa Fluor 488 (see Materials and methods for details).

ratio of NF-κB in the nucleus and cytoplasm was between 2- and 2.5-fold (Table II).

Discussion

The ß-cell uptake and metabolism of glucose leads to the closure of ATP-sensitive K^+ channels, depolarization of the plasma membrane, and subsequently, influx of Ca^{2+} through VDCCs. The Ca^{2+} signal provided by this influx of Ca^{2+} is accompanied by the release of Ca^{2+} from the endoplasmic reticulum. The subsequent increase in the $[Ca^{2+}]_i$ is an important determinant for insulin granule exocytosis. The increase

in $[Ca^{2+}]_i$ triggers direct interaction between exocytotic proteins situated in the insulin-containing granule membrane and those localized in the plasma membrane that initiates the fusion of insulin-containing granules with the plasma membrane, i.e. insulin exocytosis (5,31). The regulation of VDCC activity in ß-cells is crucial to provide an optimal concentration of Ca^{2+} in these cells. Dysfunctions in VDCC regulation can result in type 1 and type 2 diabetes.

In a cellular milieu, the protein-protein interactions provide the foundation for the formation of complex molecular architecture and networks that in turn constitute various cellular signaling pathways. The VDCC subunits not only form Ca^{2+} conducting pores in the plasma membrane, but also interact with many other proteins to form complex molecular networks. In these networks, VDCCs no longer respond only to voltage depolarization but are also modulated by their interacting partners. The VDCC subunits can even function as nonchannel proteins by cross-talk with other signaling molecules. The immunoprecipitation of ω-CTX GVIA binding proteins by using antibodies directed against syntaxin or synaptotagmin shows protein-protein interaction between VDCC and exocytotic proteins (32,33). By using fluorescence microscopy along with deconvolution analysis it was shown that the expressed CaV1.3 subunit-enhanced green fluorescent protein (GFP) and enhanced blue fluorescent protein-syntaxin 1 were targeted to and colocalized in the ß-cell plasma membrane (34). The confocal fluorescence microscopy results presented in Fig. 1 in the present study show that VDCCs interact with CaR in ß-cells exposed to TNF-α. This observation was further strengthened by the increase in the colocalization correlation coefficient as shown in Table I, that indicated a value of 175% in 20 ng/ml TNF-α-treated ß-cells as opposed to the control ß-cells. The correlation plots (see Fig. 2) showing interaction between red pixels representing CaR on the Y-axis and green pixels representing VDCC on the X-axis is another important visual demonstration of such protein-protein interactions induced by the inflammatory cytokine TNF-α in insulin producing ß-cells.

Cytokines can alter the phenotype of VDCC in ß-cells and it is tempting to investigate how cytokines selectively turn on the expression of ß-cell CaV3 channels in type 1 diabetes situation. VDCCs as a constituent of Ca^{2+} handling molecular networks play a critical role in the spatio-temporal regulation of $[Ca^{2+}]_i$ in the ß-cell (7). The glucose metabolism that leads to an influx of Ca^{2+} results in the of activation Ca^{2+} handling molecular networks in the ß-cell leading to the generation of complex $[Ca^{2+}]_i$ signals (35,36). An appropriate range of $[Ca^{2+}]_i$ is crucial for the functioning of ß-cells. Ca^{2+} signals in ß-cells can activate the transcription factor NF-κB, involved in the regulation of cell cycle and apoptosis (37). TNF-α is a cytokine widely known to activate NF-κB transcription in ß-cells (23-25). NF-κB is usually stored in the cytosol in its inactive form, bound to the inhibitory unit IκBα, which prevents DNA binding and nuclear translocation. NF-κB activating agents initiate phosphorylation of IκBα, inducing polyubiquitination at multiple sites and tagging the subunit for degradation by a 26S proteosome complex (23-25). The confocal fluorescence microscopy data presented in Fig. 5 clearly indicate that TNF-α addition to RIN cells resulted in the increased translocation of NF-κB from the cytoplasm to the nucleus. This visual observation is further substantiated by the increase in the ratio of integrated fluorescence intensities of NF-κB in the nucleus and the cytoplasm (see Table II) indicating a more than 3-fold increase in this ratio in TNF-α-treated ß-cells.

The $[Ca^{2+}]_i$ is also an important indicator of cell viability (38-41). In normal physiological conditions, the proper regulation of $[Ca^{2+}]_i$ by various constituents of Ca^{2+} handling networks maintains ß-cell growth, proliferation, and differentiation. However, in pathophysiological situations, the changes in the intracellular and/or extracellular environment can lead to dysregulation of $[Ca^{2+}]_i$ due to the altered functioning of the Ca^{2+} handling molecular networks which can cause ß-cell death (3,4,35,42). It has been shown that the addition of interferon-γ and TNF-α increases high-voltage activated (HVA) Ca^{2+} currents, markedly increasing the $[Ca^{2+}]_i$ and resulting in apoptotic death in insulin-secreting cell lines. In type 1 diabetes, the loss of pancreatic ß-cells occurs whereas in type 2 diabetes the progressive loss of ß-cell function as well as increased ß-cell apoptosis has been observed (43). The hyperactivation of ß-cell VDCC plays an important role in ß-cell apoptosis (3,4,35,42). ß-cell VDCCs could therefore be potential therapeutic targets for the prevention of ß-cell apoptosis and necrosis during the development of diabetes.

The interaction between G proteins and VDCC that leads to the inhibition of VDCC is a well-characterized mechanism of VDCC regulation that is voltage-dependent and membrane delimited. The results presented in Table I and Figs. 3 and 4 further demonstrate that the interaction between CaR and VDCC is dependent upon VDCC activity since the addition of NIMO, a blocker of L-type VDCC, significantly reduced spatial interaction between CaR and VDCC and the pretreatment of ß-cells with NIMO followed by the application of 10 ng/ml TNF-α significantly abolished such molecular interaction as evidenced by the finding that the correlation coefficient value was 0 (see Table I, Figs. 3 and 4). VDCC regulation by the direct membrane-delimited interaction with G protein leads to a positive shift in the voltage dependence and a slowing of channel activation (44). In addition to the direct regulation of VDCC by G proteins, GPCR activation also initiates a number of intracellular signaling pathways such as i) activation or inhibition of adenylyl cyclase resulting in elevation or lowering in intracellular cAMP levels, and eventually increase or decrease in protein kinase A (PKA) activity, ii) phospholipase C activation, generation of diacylglycerol (DAG) and inositol-triphosphate (InsP3), DAG and InsP3-released Ca^{2+} serving as endogenous activators of PKC, and iii) $G\alpha_{i/o}$- or Go-mediated activation of tyrosine kinases. All these protein kinases regulate VDCC (45), and $[Ca^{2+}]_i$ can directly modulate VDCC (46).

The activation of GPCR presumably involves conformational changes of the membrane-spanning helices that change the conformation of intracellular loops and C-terminus, and thereby promote activation of G proteins. The C-terminus of CaR is involved in a positively co-operative response to Ca^{2+} (47), and binding to a scaffold protein, filamin-A (48). The CaR signals via $G\alpha_i$, $G\alpha_q$, and $G\alpha_{12/13}$ proteins. Several CaR-interacting proteins such as filamin, a potential scaffolding

protein, potassium channels, signaling proteins, chaperone and trafficking proteins, and receptor activity modifying proteins (RAMPs) may lead to the regulatory functioning of CaR (17-20). GPCRs have four domains that are exposed to the intracellular space and that are available to interact with other proteins, three intracellular loops that connect transmembrane domains and the C-terminus. The intracellular loops may interact with G proteins as well as other proteins including proteins involved in signaling, such as the arrestins or spinophilin (10). The C-terminus of the CaR has been shown to interact with and inactivate two inwardly rectifying K channels, Kir4.1 and Kir4.2, in the kidney that are expressed in the distal nephron as well as other tissues (21,50-54). The findings described in the present study further strengthen the premise that CaR is able to interact with VDCC spatially. The interaction of CaR with ion channels, including VDCCs, in tissues could allow control over channel activity through direct protein-protein contact.

Acknowledgements

The author acknowledges the Florida International University Foundation's Faculty Research Award 2007-2008 by the Office of Provost and Office of Sponsored Research Administration (OSRA-FIU).

References

1. Maedler K, Storling J, Sturis J, *et al*: Glucose- and interleukin-1ß-induced ß-cell apoptosis requires Ca^{2+} influx and extracellular signal-regulated kinase (ERK) 1/2 activation and is prevented by a sulfonylurea receptor 1/inwardly rectifying K^+ channel 6.2 (SUR/Kir6.2) selective potassium channel opener in human islets. Diabetes 53: 1706-1713, 2004.
2. Zaitsev SV, Appelskog IB, Kaplioukh IL, Yang SN, Kohler M, Efendic S and Berggren PO: Imidazoline compounds protect against interleukin 1ß-induced ß-cell apoptosis. Diabetes 50: S70-S76, 2001.
3. Chang I, Cho N, Kim S, *et al*: Role of calcium in pancreatic islet cell death by IFN-γ/TNF-α. J Immunol 172: 7008-7014, 2004.
4. Wang L, Bhattacharjee A, Zuo Z, Hu F, Honkanen RE, Berggren PO and Li M: A low voltage-activated Ca^{2+} current mediates cytokine-induced pancreatic ß-cell death. Endocrinology 140: 1200-1204, 1999.
5. Yang SN and Berggren PO: ß-cell CaV channel regulation in physiology and pathophysiology. Am J Physiol 288: E16-E28, 2005.
6. Sher E, Giovannini F, Codignola A, *et al*: Voltage-operated calcium channel heterogeneity in pancreatic ß-cells: physiopathological implications. J Bioenerg Biomembr 35: 687-696, 2003.
7. Berggren PO and Larsson O: Ca^{2+} and pancreatic ß-cell function. Biochem Soc Trans 22: 12-18, 1994.
8. Hofer AM and Brown EM: Extracellular calcium sensing and signaling. Nat Rev Mol Cell Biol 4: 530-538, 2003.
9. Kifor O, Kifor I, Moore FD Jr, Butters RR Jr and Brown EM: m-Calpain colocalizes with calcium-sensing receptor (CaR) in caveolae in parathyroid cells and participates in degradation of the CaR. J Biol Chem 278: 31167-31176, 2003.
10. Brown EM, Gamba G, Riccardi D, *et al*: Cloning and characterization of an extracellular Ca^{2+} - sensing receptor from bovine parathyroid. Nature 366: 575-580, 1993.
11. Brown EM and MacLeod RJ: Extracellular calcium sensing and extracellular calcium signaling. Physiol Rev 81: 239-287, 2000.
12. Kato M, Doi R, Imamura M, Furutani M, Hosotani R and Shimada Y: Calcium-evoked insulin release from insulinoma cells is mediated via calcium sensing receptor. Surgery 122: 1203-1211, 1997.
13. Leech CA and Habener JF: A role for Ca^{2+}- sensitive non-selective cation channels in regulating the membrane potential of pancreatic ß-cells. Diabetes 47: 1066-1073, 1998.
14. Squires PE, Harris TE, Persaud SJ, Curtis SB, Buchan AMJ and Jones PJ: The extracellular calcium sensing receptor on human ß-cells negatively modulates insulin secretion. Diabetes 49: 409-417, 2000.
15. Kato M, Doi R, Imamura M, Okada N, Shimada Y, Hosotani R and Miyazaki JI: Response of human insulinoma cells is different from normal ß cells. Dig Dis Sci 43: 2429-2438, 1998.
16. Rasschaert J and Malaisse WJ: Expression of the calcium sensing-sensing receptor in pancreatic islet ß-cells. Biochem Biophys Res Commun 264: 615-618, 1999.
17. Rebois RV and Hebert TE: Protein complexes involved in heptahelical receptor-mediated signal transduction. Receptors Channels 9: 169-194, 2003.
18. Drake MT, Shenoy SK and Lefkowitz RJ: Trafficking of G protein-coupled receptors. Circ Res 99: 570-582, 2006.
19. Wang Q and Limbird LE: Regulation of α2AR trafficking and signaling by interacting proteins. Biochem Pharmacol 73: 1135-1145, 2007.
20. Enz R: The trick of the tail: protein-protein interactions of metabotropic glutamate receptors. Bioessays 29: 60-73, 2007.
21. Huang C, Sindic A, Hill CE, *et al*: Interaction of the Ca-sensing receptor with the inwardly-rectifying potassium channels Kir4.1 and Kir4.2 results in inhibition of channel function. Am J Physiol Renal Physiol 292: F1073-F1081, 2007.
22. Parkash J, Chaudhry MA and Rhoten WB: Tumor necrosis factor-α induced changes in insulin-producing ß-cells. Anat Rec 286A: 982-993, 2005.
23. Flodstrom M, Welsh N and Eizirik DL: Cytokines activate the nuclear factor κB (NF-κB) and induce nitric oxide production in human pancreatic islets. FEBS Lett 385: 4-6, 1996.
24. Sekine N, Ishikawa T, Okazaki T, Hayashi M, Wollheim CB and Fujita T: Synergistic activation of NF-κB and inducible isoform of nitric oxide synthase induction by interferon-gamma and tumor necrosis factor-alpha in INS-1 cells. J Cell Physiol 184: 46-57, 2000.
25. Stephens LA, Thomas HE, Ming L, Grell M, Darwiche R, Volodin L and Kay TW: Tumor necrosis factor-alpha-activated cell death pathways in NIT-1 insulinoma cells and primary pancreatic beta cells. Endocrinology 140: 3219-3227, 1999.
26. Donath MY and Halban PA: Decreased ß-cell mass in diabetes: significance, mechanisms and therapeutic implications. Diabetologia 47: 581-589, 2004.
27. Ortis F, Cardozo AK, Crispim D, Storling J, Mandrup-Poulsen T and Eizirik DL: Cytokine-induced proapoptotic gene expression in insulin-producing cells is related to rapid, sustained, and non-oscillatory nuclear factor-kappaB activation. Mol Endocrinol 20: 1867-1879, 2006.
28. Wajant H, Pfizenmaier K and Scheurich P: Tumor necrosis factor signaling. Cell Death Differ 10: 45-65, 2003.
29. Costes SV, Daelemans D, Cho EH, Dobbin Z, Pavlakis G and Lockett S: Automatic and quantitative measurement of protein-protein colocalization in live cells. Biophys J 86: 3993-4003, 2004.
30. Manders EMM, Verbeek FJ and Aten JA: Measurement of co-localization of object in dual-colour confocal images. J Microsc 169: 375-382, 1993.
31. Yang SN and Berggren PO: CaV2.3 channel and PKC: new players in insulin secretion. J Clin Invest 115: 16-20, 2005.
32. Bennett MK, Calakos N and Scheller RH: Syntaxin: a synaptic protein implicated in docking of synaptic vesicles at presynaptic active zones. Science 257: 255-259, 1992.
33. Leveque C, Hoshino T, David P, *et al*: The synaptic vesicle protein synaptotagmin associates with calcium channels and is a putative Lambert-Eaton myasthenic syndrome antigen. Proc Natl Acad Sci USA 89: 3625-3629, 1992.
34. Yang SN, Larsson O, Branstrom R, *et al*: Syntaxin 1 interacts with the L_D subtype of voltage-gated Ca^{2+} channels in pancreatic ß-cells. Proc Natl Acad Sci USA 96: 10164-10169, 1999.
35. Juntti-Berggren L, Larsson O, Rorsman P, *et al*: Increased activity of L-type Ca^{2+} channels exposed to serum from patients with type I diabetes. Science 261: 86-90, 1993.
36. Efanova IB, Zaitsev SV, Zhivotovsky B, Kohler M, Efendic S, Orrenius S and Berggren PO: Glucose and tolbutamide induce apoptosis in pancreatic ß-cells. A process dependent on intracellular Ca^{2+} concentration. J Biol Chem 273: 33501-33507, 1998.
37. Bernal-Mizrachi E, Wen W, Shornick M and Permutt MA: Activation of nuclear factor-κB by depolarization and Ca^{2+} influx in MIN6 insulinoma cells. Diabetes 51: S484-S488, 2002.

38. Berridge MJ, Bootman MD and Lipp P: Calcium: a life and death signal. Nature 395: 645-648, 1998.
39. Berridge MJ, Lipp P and Bootman MD: The versatility and universality of calcium signalling. Nat Rev Mol Cell Biol 1: 11-21, 2000.
40. Berridge MJ, Bootman MD and Roderick HL: Calcium signalling: dynamics, homeostasis and remodelling. Nat Rev Mol Cell Biol 4: 517-529, 2003.
41. Orrenius S, Zhivotovsky B and Nicotera P: Regulation of cell death: the calcium-apoptosis link. Nat Rev Mol Cell Biol 4: 552-565, 2003.
42. Juntti-Berggren L, Refai E, Appelskog I, *et al*: Apolipoprotein CIII promotes Ca^{2+} dependent ß-cell death in type 1 diabetes. Proc Natl Acad Sci USA 101: 10090-10094, 2004.
43. Mathis D, Vence L and Benoist C: ß-cell death during progression to diabetes. Nature 414: 792-798, 2001.
44. Dolphin AC: G protein modulation of voltage-gated calcium channels. Pharmacol Rev 55: 607-627, 2003.
45. Strock J and Diverse-Pierluissi MA: Ca^{2+} channels as integrators of G protein-mediated signaling in neurons. Mol Pharmacol 66: 1071-1076, 2004.
46. Isaev D, Solt K, Gurtovaya O, Reeves JP and Shirokov R: Modulation of the voltage sensor of L-type Ca^{2+} channels by intracellular Ca^{2+}. J Gen Physiol 123: 555-571, 2004.
47. Gama L and Breitwieser GE: A carboxyl-terminal domain controls the cooperativity for extracellular Ca^{2+} activation of the human calcium sensing receptor. A study with receptor-green fluorescent protein fusions. J Biol Chem 273: 29712-29718, 1998.
48. Hjalm G, MacLeod RJ, Kifor O, Chattopadhyay N and Brown EM: Filamin-A binds to the carboxyl-terminal tail of the calcium-sensing receptor, an interaction that participates in CaR-mediated activation of mitogen-activated protein kinase. J Biol Chem 276: 34880-34887, 2001.
49. Lourdel S, Paulais M, Cluzeaud F, *et al*: An inward rectifier K^+ channel at the basolateral membrane of the mouse distal convoluted tubule: similarities with Kir4-Kir5.1 heteromeric channels. J Physiol 538: 391-404, 2002.
50. Ito M, Inanobe A, Horio Y, *et al*: Immunolocalization of an inwardly rectifying K channel, KAB-2 (Kir4.1), in the basolateral membrane of renal distal tubular epithelia. FEBS Lett 388: 11-15, 1996.
51. Ookata K, Tojo A, Suzuki Y, Nakamura N, Kimura K, Wilcox CS and Hirose S: Localization of inward rectifier potassium channel Kir7.1 in the basolateral membrane of distal nephron and collecting duct. J Am Soc Nephrol 11: 198-94, 2000.
52. Riccardi D, Hall AE, Chattopadhyay N, Xu JZ, Brown EM and Hebert SC: Localization of the extracellular Ca^{2+}/polyvalent cation-sensing protein in rat kidney. Am J Physiol. 274: F611-F622, 1998.
53. Yoshitomi K, Shimizu T, Taniguchi J and Imai M: Electrophysiological characterization of rabbit distal convoluted tubule cell. Pflugers Arch 414: 457-463, 1989.
54. Pessia M, Imbrici P, D'Adamo MC, Salvatore L and Tucker SJ: Differential pH sensitivity of Kir4.1 and Kir4.2 potassium channels and their modulation by heteropolymerization with Kir5.1. J Physiol 532: 359-367, 2001.